Doppler Back-scattering diagnostic in the TCV tokamak

P. Molina Cabrera, S. Coda, L. Porte, A. Smolders, N. Offeddu,
P. Lavanchy, M. Silva, M. Toussaint, and the TCV team [1]
Swiss Plasma Center, École Polytechnique Fédérale de Lausanne (EPFL), CH-1015 Lausanne, Switzerland.

The present proceeding describes the design and latest results of a new continuous-wave V-band Doppler back-scattering (DBS) diagnostic developed at the TCV tokamak. Prototype microwave reflectometers and DBS systems had been tested in TCV in the past, on loan from collaborators from the University of Stuttgart, Forschungszentrum Jülich, and the Laboratoire de Physique des Plasmas of École Polytechnique Palaiseau. However, the DBS system described here is the first effort to build a *dedicated* DBS diagnostic for TCV with long-term exploitation goals in mind. DBS is an active diagnostic technique that allows the study of electron density turbulence via the scattering of an electromagnetic beam launched at oblique incidence to a cut-off layer. DBS takes advantage of the enhanced E-field amplitude near a plasma cut-off and the presence of a broad wave-number spectrum of electron density fluctuations to efficiently scatter these waves. By measuring the Doppler shift and power of the scattered radiation,the perpendicular velocity and wave number spectrum of density fluctuations can be inferred.

2D 3-point ray-tracing simulations are used to estimate the backscattering location (r) and effecive $k_\perp$ as well as uncertainties as outlined in [2]. Since the V-band often finds cut-offs in the 'edge' region (ρ_ψ 0.8-1.0) of TCV plasmas, an accurate model of the scrape-off-layer (SOL) density profile is paramount to correctly estimate r and $k_\perp$. The SOL density profile is obtained from reciprocating probe measurements [3]. Comparing ray-tracing simulations with and without SOL profile concluded that if the $k_\perp$ measured is above 8 cm^{-1} and/or has turning points above ρ_ψ 0.95, the beam's refraction inside the SOL plays an important role in the accuracy of wavenumber estimates [4]. The available $k_\perp$ range is found between 3 and 16 cm^{-1} with a resolution of 2-4 cm^{-1}. A flexible quasi-optical launcher antenna [5] allows poloidal (10-55^o) and toroidal (360^o) steering of the beam with 0.2^o accuracy. A pair of motorized HE_{11} miter-bend polarizers allow flexible coupling to either O or X mode and programmable polarization changes during the shot. The instrument can thus sample plasmas with densities 0.8 to $7\times10^{19}m^{-3}$. This proceeding begins by briefly presenting the hardware setup of both single and multi-frequency DBS systems. Initial results are then discussed, closing with polarization rotation experiments attempting to measure the edge B-field line pitch. Further details can be found in [4, 6].

Swept single-frequency hardware set-up

TCV's DBS diagnostic is capable of swept single and multi frequency operation through two interchangeable setups as described below. The first, more conventional approach, uses a heterodyne transceiver (Tx/Rx) and an I/Q mixer as shown in figure 1. At the core sits a commercial off-the-shelf trasceiver VNA extension module from Virginia Diodes (VDI). The main oscillator, providing synchronized RF and local-oscillator frequencies is a 25GHz analog band-width arbitrary waveform generator (AWG) Keysight M8195SA. It produces 4dBm 8.3-12GHz sinusoids which are brought into the V-band by x6 varactor multipliers inside the Tx/Rx module. The intermediate frequency chosen was 1.88GHz to permit easy amplification while ensuring minimal interference from spurious signals. Upon downconversion, the reflected power is amplified (30dB) and band-pass filtered (60MHz BW) before being fed into an I/Q mixer which is used to extract amplitude and phase from the reference and measured signals. The I/Q signals are routed from the DBS box to the digitizer through shielded twisted pair cables which are balanced and hence resilient against changing E fields. The I/Q signals are then sampled by a 14-bit differential ADC at 4MHz.

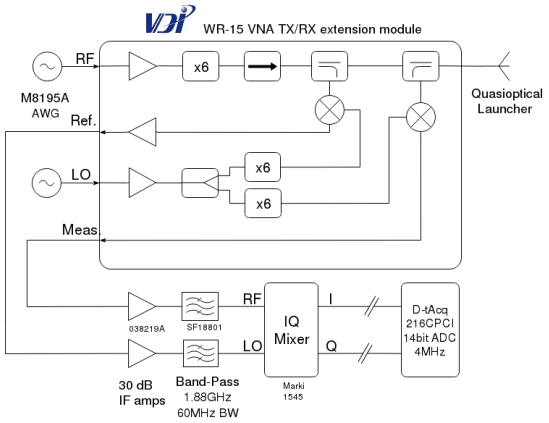

Figure 1: Block diagram of the sweepable single-frequency DBS implementation

Swept multi-frequency hardware set-up

A new approach for the production and detection of multiple simultaneous frequencies has been developed and tested. It consists of creating a double frequency spectrum with an AWG, feeding this signal into the varactor multipliers inside the VNA extension module above, and directly sampling the entire output spectrum with a fast oscilloscope. It is known [7, p.513] that the response of frequency multipliers to a double frequency input is the generation of intermodulation frequency products of the form $nf1 + mf2$. Therefore, if a two-tone input composed of f1 and f2 is fed into the x6 VDI varactor multiplers, their output would consist of

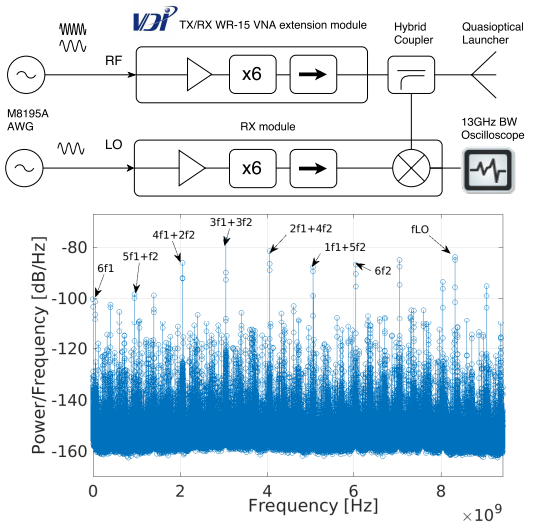

Figure 2: Top: Block diagram of the multi-channel DBS setup. Bottom: raw IF PSD spectra showing the main multiplication and intermodulation terms.

6f1, 6f2, and 5 other intermodulation products in between, as shown in figure 2. The separation between these products corresponds to the initial frequency difference f1-f2. Seven frequencies can thus be sent into the plasma. The total span of these frequencies is only limited by the bandwidth of the receiver (10GHz in this case). A fast 13GHz analog bandwidth oscilloscope (Lecroy Wavemaster 813Zi-B) is used to directly sample the IF output of the receiver mixer. This new approach to multi-channel DBS has both advantages and disadvantages. Firstly, the non-linear-transmission-lines (NLTL) of comb-frequency generators [8, 9] are not required. Furthermore, the fixed filter banks in the receiver are all substituted by the fast scope which records the Doppler shifts of each frequency simultaneously. Also, the multi-frequency range and spacing can be arbitrarily changed by varying the bi-frequency AWG input. This can prove very useful in radial correlation studies [10]. A disadvantage of the current approach is that the plasma can be sampled for a maximum of 2ms given the limited scope memory at 32Mb. This limitation can be overcome by data-acquisition solutions that feature memories of several 10s of gigabytes (i.e. Guzik ADP7000). Another limitation is that the power dependence on frequency follows a near-parabolic curve, which complicates radial turbulence level studies yet can be corrected via a power calibration.

Results and discussion

Perpendicular rotation velocity estimates compare well against ExB plasma poloidal rotation estimates from CXRS as can be seen in figure 3. The lack of agreement, specially in the H-mode case, can be attributed to the fact that the DBS diagnostic measures from a upper-lateral port at the top right corner of the plasma while the CXRS diagnostic measures at the plasma equator. Poloidal rotation velocities asymmetries have been reported in other tokamaks [11]. Data from plasma discharges 59551-53 has validated the multi-channel technique by using separations of 0.5, 1, and 2 GHz which agree with each other, regular I/Q DBS, as well as with ExB estimates from CXRS [4].

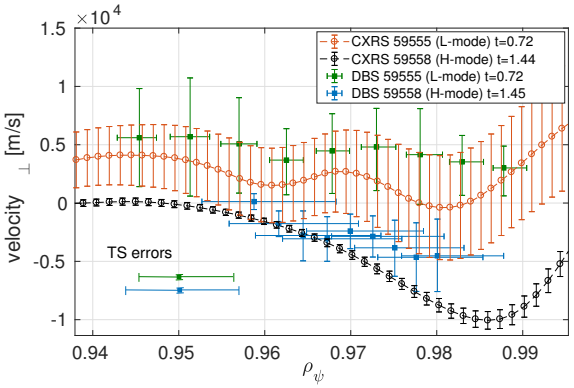

Figure 3: Comparing DBS perpendicular turbulence velocity estimates with CXRS v_{ExB} estimates in L-mode (59555, $k_\perp$ 5-5.8 cm^{-1}) and H-mode (59558, $k_\perp$ 6.5-7.5 cm^{-1}) discharges. The average TS contribution to $\Delta\rho_\psi$ and Δv are shown decoupled from the inherent DBS uncertainties for illustrative purposes.

Polarization rotation inside the shot

Another unique capability of TCV's DBS system is the in-shot polarization rotation of the outgoing beam. A pair of 63.5mm circular 1970s, he became a born-again Christian and released a series of albums of contemporary gospel music before returning to his corrugated waveguide motorized polarizer miter bends have been used to change the inclination angle of the polarization ellipse α while keeping a constant elliptical polarization angle β in search of an independent measurement of the magnetic field-line pitch. The best coupling to either X or O mode can be calculated by matching the launched beam wavevector and polarization to the relevant mode in the plasma's LCFS based on the magnetic field reconstruction. The coupling of the launched wave to either X or O mode at the plasma LCFS could be made to change by varying α while keeping β constant. If both the effective α and the power of the DBS signal during the shot are examined, a measurement of the magnetic field pitch angle at the edge of the plasma is possible. Figure 4 shows time traces of both α and β angles during shot 59679. The encoder output of both linear and elliptical miter bend polarizer angles is mapped onto α and β maps over the shot time. Figure 4 shows that the effective α changes between +20 and -40 degrees while β can be made to remain between -5 and -6 degrees , aiming for an ideal -5.36 degrees for X-mode best coupling at a chosen toroidal angle of 0 degrees. The best coupling to the X-mode wave into the main plasma should occur when the probing beam's α is perpendicular to the LCFS B-field line.

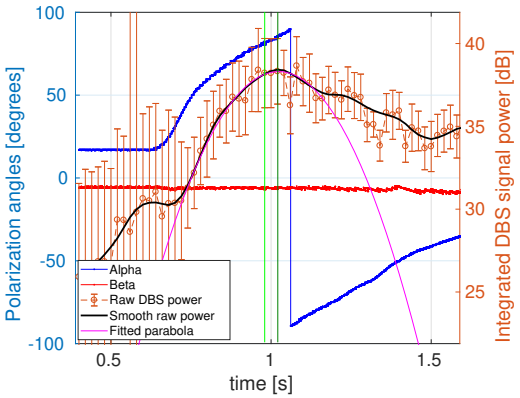

Figure 4: DBS signal power evolution over changing polarization axis inclination (α) angle: i.e. coupling into X/O-mode. 20ms time windows are taken for each PSD estimate, which leads to a 20ms DBS power signal. Shot 59679. Output frequency was 60GHz. Poloidal and toroidal angles are 18 and 0 degrees respectively. X-mode turning point at ρ_ψ=0.97 $\pm$ 0.01 with $k_\perp$= 8.2 $\pm$2 cm^1. O-mode turning point expected at ρ_ψ=0.89 $\pm$0.01 with $k_\perp$=10.5$\pm$2cm^{-1}. Dark green vertical line shows the peak integrated DBS signal power and the light green shows the LIUQE estimate of where such peak should have happened. DBS signal power evolution over changing polarization axis inclination (α) angle during shot 59679.

The DBS signal power is estimated by integrating the area under the fits to the smooth DBS PSD spectra. A parabola is fit to the points around the peak power to determine the time of the peak DBS signal power. This peak is found at time 1.02 $\pm$ 0.01 where the alpha angle was 84.5 $\pm$ 3. The best X-mode coupling α estimate agrees within uncertainty with the LIUQE suggestion of 81.7$\pm$ 0.4^o. Although agreement within error bars is found, it can be concluded

that the current lower-bound experimental uncertainty of $\pm 3^o$ must decrease by at least an order of magnitude to make this method practically relevant. This can be achieved by optimizing the motor's trajectory for speed and increased symmetry in the α scan. A repair to the elliptical unit showing signs of increased torque is foreseen in the near future in order to continue these experiments.

Acknowledgments

This work is partially supported by Requip grant (No. 206021-150707) of the Swiss National Science Foundation and by the Helmholtz Virtual Institute on Plasma Dynamical Processes and Turbulence Studies using Advanced Microwave Diagnostics. This work has been carried out within the framework of the EUROfusion Consortium and has received funding from the Euratom research and training programme 2014-2018 under grant agreement No 633053. The views and opinions expressed herein do not necessarily reflect those of the European Commission.

References

[1] S. Coda. Physics Research on the TCV Tokamak Facility: From Conventional To Alternative Scenarios and Beyond. *Nuclear Fusion*, 59(112023), 2019.

[2] G.D. Conway, C. Lechte, and A. Fochi. Assessment of Doppler reflectometry accuracy using full-wave codes with comparison to beam-tracing and analytic expressions. In *12th International Reflectometry Workshop*, number May 18-20, pages 1–14, 2015.

[3] N. Vianello, C. Tsui, C. Theiler, S. Allan, J. Boedo, B. Labit, H. Reimerdes, K. Verhaegh, W. A.J. Vijvers, N. Walkden, S. Costea, J. Kovacic, C. Ionita, V. Naulin, A. H. Nielsen, J. Juul Rasmussen, B. Schneider, R. Schrittwieser, M. Spolaore, D. Carralero, J. Madsen, B. Lipschultz, and F. Militello. Modification of SOL profiles and fluctuations with line-average density and divertor flux expansion in TCV. *Nuclear Fusion*, 57(11), 2017.

[4] P. Molina Cabrera, S. Coda, L. Porte, N. Offeddu, P. Lavanchy, M. Silva, and M. Toussaint. V-band Doppler backscattering diagnostic in the TCV tokamak. *Review of Scientific Instruments*, 89(8):083503, 2018.

[5] T. P. Goodman, V. S. Udintsev, I. Klimanov, A. Mueck, O. Sauter, and C. Schlatter. First measurements of oblique ECE with a real-time movable line of sight on TCV. *Fusion Science and Technology*, 53(1):196–207, 2008.

[6] P. Molina Cabrera. *Tokamak plasma edge studies by microwave short-pulse reflectometry and backscattering.* Ph.d. thesis, Ecole Polytechnique Federale de Lausanne, 2019.

[7] David M. Pozar. *Microwave Engineering*. Addison-Wesley Publishing Company Inc., Reading, Massachusets, 1993.

[8] W. A. Peebles, T. L. Rhodes, J. C. Hillesheim, L. Zeng, and C. Wannberg. A novel, multichannel, comb-frequency Doppler backscatter system. *Review of Scientific Instruments*, 81(10), 2010.

[9] R. Soga, T. Tokuzawa, K. Y. Watanabe, K. Tanaka, I. Yamada, S. Inagaki, and N. Kasuya. Developments of frequency comb microwave reflectometer for the interchange mode observations in LHD plasma. *Journal of Instrumentation*, 11(2), 2016.

[10] J Pinzón, T Estrada, T Happel, P Hennequin, E Blanco, and U Stroth. Measurement of the tilt angle of turbulent structures in magnetically confined plasmas using Doppler reflectometry. *Plasma Phys. Contr. Fusion*, 61(105009):17pp, 2019.

[11] L. Vermare, P. Hennequin, D. Gürcan, X. Garbet, C. Honoré, F. Clairet, J. C. Giacalone, P. Morel, and A. Storelli. Poloidal asymmetries of flows in the Tore Supra tokamak. *Physics of Plasmas*, 25(2), 2018.